



Volume XXV 2022

ISSUE no.2

MBNA Publishing House Constanta 2022



Scientific Bulletin of Naval Academy

SBNA PAPER • **OPEN ACCESS**

Aspects regarding environmental and atmospheric monitoring with unmanned aerial vehicles

To cite this article: V. PRISACARIU, A. PITICAR, A. STOICULETE, *Scientific Bulletin of Naval Academy*, Vol. XXV 2022, pg. 88-99.

Submitted: 14.05.2022

Revised: 26.09.2022

Accepted: 17.10.2022

Available online at www.anmb.ro

ISSN: 2392-8956; ISSN-L: 1454-864X

doi: 10.21279/1454-864X-22-I2-009

SBNA© 2022. This work is licensed under the CC BY-NC-SA 4.0 License

Aspects regarding environmental and atmospheric monitoring with unmanned aerial vehicles

^{1a}Vasile PRISACARIU, ^{1b}Adrian PITICAR, ^{2c}Adrian STOICULETE

¹*Henri Coandă* Air Force Academy, Braşov, Romania,

² Carol I Naţional Defence University, Bucureşti, Romania

^aprisacariu.vasile@afahc.ro,

^bpiticar.adrian@afahc.ro

^cstoiculete.adrian@yahoo.com

Abstract

Anthropogenic activities produce global changes on a global scale, which has led to focused efforts on funding and adopting global monitoring programs to obtain relevant information through a series of optimized micro-scale techniques on a global scale (satellite observations). In order to obtain a complete picture of the terrestrial geo-system, efforts are being made to identify, collect and process atmospheric and environmental data using fixed, mobile, terrestrial, aerial, aquatic and orbital technical systems.

The paper sets out a number of theoretical and applied issues (proposed airplane system) relevant to sampling atmospheric and environmental data, including technologies for taking unmanned aerial vehicle data and specific equipment.

Keywords: *environmental parameters, sensors, UAS, XFRL5, conceptual design*

Acronyms and symbols

AoA	Angle of attack	C3	Command, control, and communications
CNRN	Chemical, biological, radiological and nuclear	IoT	Internet of Things
MEMS	Micro Electronic Mechanical Systems	MOX	Metal-oxide
NDVI	Normalized Difference Vegetation Index	PID	Photo-ionization detection
PM	Particulate matter	RH	Relative humidity
LoRaWAN	Low Power, Wide Area	NDIR	Non-dispersive infrared
TSFC	Thrust-specific fuel consumption	VOC	Volatile organic compound
WLAN	Wireless Local Area Network	L, D	Lift, drag (aerodynamic forces)
E	Endurance	R	Range
c_o/c_e	Root / tip	V_{TO}	Speed take-off
c_L, c_D	Lift coefficient / drag coefficient	ppm/b	parts per million/bilion
ρ	Air density	W, W_i , W_f	Weight, initial/final

1. Introduction

In the modern days meteorological and environmental observations increased exponentially. Scientific knowledge about the atmospheric behaviour and environment plays a critical role in the safeguarding of life, agriculture and infrastructure [1]. Thus, increasing sources of observations is essential in order to develop a more complete understanding of weather and environment.

The ongoing development of the Unmanned Aerial Vehicles (UAVs) used for meteorological and environmental observation date back to 1960s and includes microwave sounders, infrared spectrometers and various sensors specialized in measuring specific environmental properties. Large amounts of atmospheric vertical profile observations are collected via satellite, radiosonde soundings. However, these tools do not provide the accuracy and resolution of UAVs campaigns observations which are far superior [4]. Recently, it has been shown that in-situ meteorological measurements of the atmospheric boundary layer with UAVs are a promising and usable tool for this type of measurements. Meteorological measurements carried by UAVs open opportunities for new data that could improve the understanding of atmospheric processes at topo-climate scales such as lakes, forests and urban areas [2]. UAVs meteorological observations assimilated into numerical weather prediction models revealed a substantial reduction of model bias in forecasting weather parameters [3]. For instance, UAVs observations from the Southern Ocean improved the analyses of air temperature, wind speed and humidity in the Polar version of the Weather Research and Forecasting model [4].

Furthermore, environmental monitoring via UAVs have a considerable potential to significantly improve the understanding of hydrological processes, natural and agricultural systems and to assess, forecast and prevent natural disasters [5]. Recent UAVs an environmental observation has focused on atmospheric observations, land cover mapping, vegetation state, phenology and health, disaster mapping, soil erosion, and change detection. [5]. Observations via UAVs from atmospheric, terrestrial and maritime environments provide new and flexible solutions to different users [6]. For example, air quality elements such as ozone, CO₂, CH₄, Particulate Matter (PM), NO₂, volatile organic compounds have been successfully measured [7, 8, and 9].

2. UAVs used in environmental and atmosphere monitoring

2.1. Use of UAVs in environmental protection

UAVs rewrite a number of rules in the field of environmental protection through several approaches: transport and delivery services; conservation of coastal and marine biodiversity and terrestrial ecosystems; monitoring of photovoltaic / wind farms and energy transmission systems (electricity, oil); sustainable agriculture and crop monitoring; aerial topography and reforestation.

Transport and delivery services involve low emissions and have very low effects on biodiversity (electric propulsion). UAVs can be used in biodiversity conservation by monitoring and acquiring data from areas of interest in case of emergencies (floods, earthquakes, floods) or for law enforcement (poaching).

The management of complex inspections on photovoltaic / wind farms or energy buses is done with logistical and time-consuming implications versus the case of using traditional resources (ground monitoring). UAVs provide farmers with agricultural monitoring tools for crop health assessment (NDVI index) or for phytosanitary treatment of cultivated land. Land management through aerial topography approaches can be achieved with the help of drones at low cost and the rapid identification of problem areas. Drones can perform forestry activities through reforestation through monitoring and effective seed planting, especially in hard-to-reach areas.

2.2. Types of UAVs

Recent technological innovations have allowed unmanned aircraft (at reasonable costs) to acquire accurate data with user-defined spatial resolutions using dimensionally and mass-optimized sensors, making it possible to study locations of interest, individual organisms or atmospheric changes.

The current state of UAV technologies proves a relevant level of maturity that qualifies them for various missions and geographical areas that require limit conditions of use.

Monitoring the environment (terrestrial, air and aquatic) and the atmosphere, involves the optimization of technical resources leading to a classified approach to the constructive types of UAVs, in a series of research papers, the most relevant being: airship [10, 11 and 21], rotorcopter /

multicopter [13, 14 and 16], fixed wing [16, 17, 18 and 22], or hybrid / all classes [15, 19], see Figures 2.1-2.2.



Fig. 2.1. Qinetiq Zephyr [19]



Fig. 2.2. NASA-SIERRA [22]

2.3. UAV solar powered

The fixed-wing UAVs powered by solar cells offer advantages of long range and low level sound signature. A number of studies have generated relevant results on atmospheric monitoring with this type of air vectors.

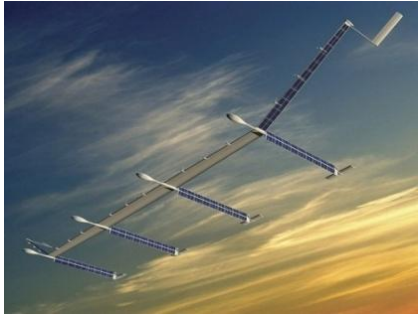


Fig. 2.3. Boeing Solar Eagle Vulture II [23]



Fig. 2.4. Boeing Solar Eagle Vulture II [23]

The most relevant in progress projects are Airbus-QinetiQ with Zephyr (see Figure 2.1); Boeing Phantom Works - Solar Eagle (see Figure 2.4); Google Titan Aerospace Solara 50; Google Skybender; Facebook Ascenta/ Aquila; AeroVironment / NASA Gossamer Albatros, Solar Challenger and NASA Pathfinder (see Figure 2.5); NASA Centurion; NASA Helios (see Figure 2.6); Bye Engineering / Bye Aerospace with Silent Falcon UAV figure 2.7, [24]; Atlantic Solar figure 2.8, [23]. Flight characteristics and performance are shown in Table 2.1.



Fig. 2.5. AeroVironment - Pathfinder [23]



Fig. 2.6. NASA – Helios [23]

Table 2.1. UAV features

Performances /Vector	Span	Speed	Payload /MTOW	Power	Ceiling	Autonomy
Zephir 8	28 m	56 km/h	5/75 kg	2x0,60CP	21.000 m	26 days
Vulture II	120 m	80 km/h	-	20x ...CP	-	5 years
Solara 60	60 m	105 km/h	100/x kg	-	20.000 m	-
Aquila	43 m	-	x/399 kg	-	27.000 m	-
Pathfinder	29,5 m	-	45/252 kg	6x ..CP	21.802 m	-
Centurion	61,8 m	33 km/h	270/870 kg	14x2CP	-	-
Silent Falcon UAV	4,27 m	112 km/h	x/13,5 kg	-	-	7 h
Atlantik Solar	5,6 m	-	x/6,3 kg	-	-	-



Fig. 2.7. Silent Falcon UAV [24]



Fig. 2.8. Atlantik Solar - UAV [23]

3. UAV sensors for environmental missions

Airborne sensors can capture real-time data and monitor atmospheric and environmental parameters (physical and chemical) in areas of interest, such as temperature, humidity, barometric pressure, radioactivity, dust particles (PM), CO, CO₂, NO₂, SO₂, O₃, NH₃, VOC. For the present study we use two types of sensors, a customized sensor: uRAD Monitor and a sensor dedicated to UAVs: Sniffer 4D.

3.1. uRADMonitor A3 air quality monitoring station

It is part of the global uRAD Monitor project that contains continuous environmental monitoring stations, generating open source data online [25, 26], variant A3 can take data for 8÷11 relevant parameters regarding air quality, see figure 3.1. There are 4 variants of A3: Ethernet, WLAN, LoraWAN, GSM.

A3 can be used in applications for monitoring household parameters, in industrial and production areas, CBRN monitoring, Smart Cities and IoT, in stationary and onboard (vehicles / airplane) configuration it has a total mass of 170g which is recommended for data collection using UAV, see the characteristics in table 3.1.

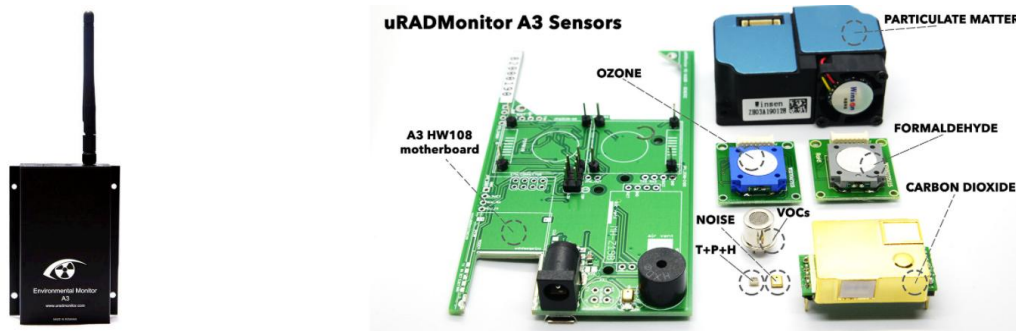


Fig. 3.1. uRAD Monitor A3 [25]

Table 3.1. uRAD Monitor A3 technical data, [25]

Parameter	Range	Resolution	Lifespan ⁽¹⁾	Detection method
Temperature	-40÷85°C	0,5°C	5 years	MEMS
Humidity	0%÷100%RH	1%RH	5 years	-
PM 1 /2.5 / 10	0÷1000µg/m ³	1µg/m ³	5 years	laser scattering
CO ₂	400÷5000 ppm	1 ppm	5 years	NDIR
CH ₂ O (formaldehida)	0 ÷5 ppm	10 ppb	2 years	electrochemical
O ₃	0 ÷10 ppm	10 ppb	2 years	electrochemical
VOCs	10 ÷1000 ppm ⁽²⁾	-	2 years	MOX
Noise	30÷130dB	1dB	2 years	analogue sound

(1) Estimated under normal conditions of use. Device maintenance is recommended after the shortest sensor life (2 years);

(2) For alcohol estimated.

3.2.Sniffer 4D

It is an integrated environmental monitoring platform containing a basic module and 9 optional modules depending on the needs of the end user, the product also comes with a dedicated software tool for the acquisition, processing and interpretation of environmental data, see figure 3.2, [28] .

The main module includes: data processing unit, telemetry system, GPS module, protection housing, temperature and humidity sensors, cooling system, power module, back-up module (SD card).



Fig. 3.2. Sniffer 4D, a. model V1, b. model V2 [28]



Fig. 3.3. Date graphics Sniffer 4D [28]

Optional modules can be: VOC, O₃ + / NO₂, CO, SO₂, VOC, C_xH_x, HCl, H₂S, H₂, NH₃, 4G transmission. Sniffer 4D can be delivered with mounting kits for DJI M 100, DJI M210, DJI M600. A selection of the relevant technical specifications are in Table 3.2.

Table 3.2. Sniffer 4D technical data [28]

Module	CPU/RAM / resolution	Weight	Life	Range	Detection method
<i>Main module</i>					
Main Unit	1GHz/ 512 Mb	350g	-	7/ 3-5 km	433MHz Radio; Telemetry system; Temp., humidity, pressure Sensor
<i>Sensor modules</i>					
PM 2.5	1ug/m ³ / 1Hz;	29 g	3 years	0~1000ug/m ³ ;	laser scattering/ light scattering
O ₃ +NO ₂	0.5 ppb/ 1Hz	20 g	2 years	0~10ppm	electrochemistry
CO	0.7 ppb/ 1Hz	20 g	3 years	0~10ppm	electrochemistry
SO ₂	0.5 ppb/ 1Hz	20 g	3 years	0~15ppm	electrochemistry
VOC	3.8 ppb/ 1Hz	11 g	5000 h	0~50ppm	PID
CxHx	100 ppb/ 1Hz	22 g	5 years	0~0,2/0,5% propane / methane	NDIR
HCl	100 ppb/ 1Hz	20 g	2 years	0~100ppm	electrochemistry
H ₂ S	1 ppb/ 1Hz	20 g	2 years	0~50ppm	electrochemistry
H ₂	0,8 ppb/ 1Hz	20 g	2 years	0~3000ppm	electrochemistry
NH ₃	1Hz	20 g	2 years	0~100ppm	electrochemistry

4. UAV concept for atmospheric and environmental monitoring

4.1. UAV mission

The aerodynamic and weight configurations of the UAV are optimized for long endurance missions in the version of the glider with internal combustion engine. Starting from the existing configurations of similar gliders, with large aspect ratio wing in the literature [12, 20, 27, and 29], we propose the aerodynamic configuration in subchapter 4.2.

4.2. UAV description

a. Aerodynamic configuration

The twin boom configuration proposal offers both structural advantages through increased rigidity and an optimized distribution on the wing and aerodynamic advantages offering the possibility of using wings with long elongation and large span which can place the air vector in high endurance UAV class (possibly short-range / mid-range).

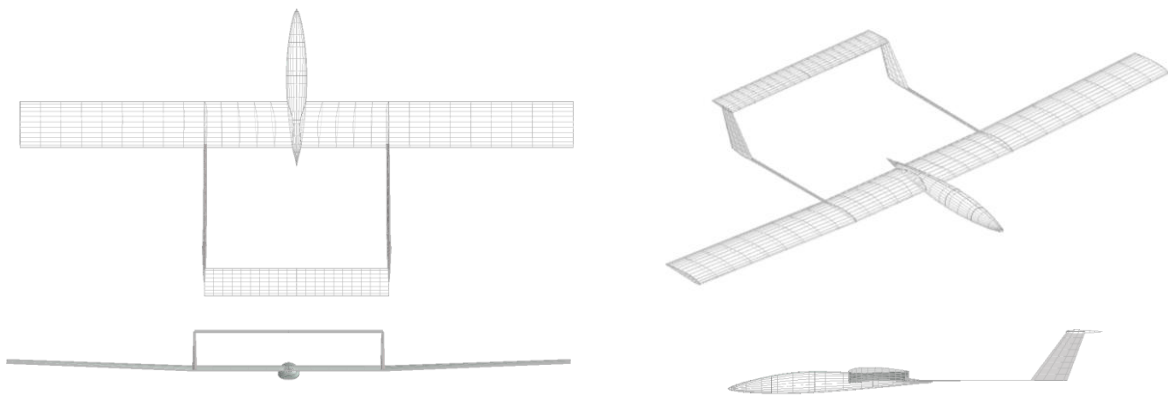


Fig 4.1 Motor glider UAV ATMOS-2CB (combustion engines)

For simplicity in construction, the variant of a rectangular lifting surface was adopted. The configuration are shown in Figure 4.1 and the geometric features in Table 4.1

Table 4.1. Estimated features ATMOS-2CB

Features	Value	Features	Value
Span (m) / Length (m)	6 / 3,1	Swept / twist angle (°)	0° / 0°
Wing area (m ²)	3,6	Dihedral angle (°)	2.5°
Aspect ratio	12	Airfoil wing / tail	NACA6409-2409 / NACA 0012
Root/tip chord c_0/c_e (m)	0,5/0,5	Propulsion	Combustion engine 1 x 1,9CP/1,42Kw

b. Airfoils

For 2D sections of the wing selected NACA 6409-NACA 2409 airfoils, and for tail selected NACA 0009 / NACA 0015 airfoils, see figure 4.2.

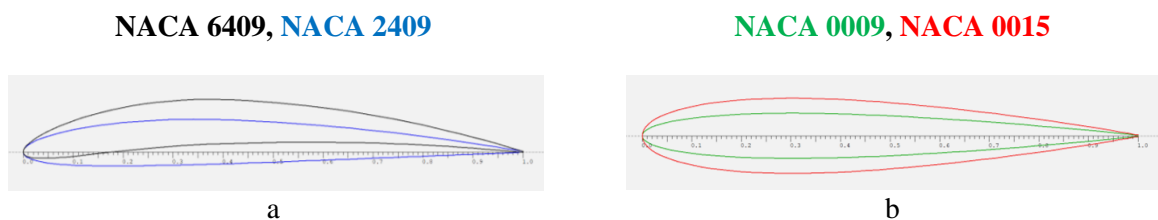


Fig. 4.2. Airfoils: a. wing, b. tail

4.3. Estimation of UAV performance with combustion engine

For an overview of the aerodynamic solution we propose the numerical estimation of the flight and propulsion performance (for the combustion engine version) as follows:

a. speeds estimation (for $W=10\text{kg}$ weight):

-speed at $C_L=0,75$ ($\text{AoA}=0^\circ$), for NACA 6409 airfoil:

$$V_\infty = \sqrt{\frac{2 \cdot W}{\rho \cdot S \cdot c_L}} = 8,4 \frac{m}{s} = 30,24 \text{ km/h} \quad (1)$$

-speed limit for $C_{Lmax}=1,77$ ($\text{AoA}=9^\circ$ and flap at 25°):

$$V_{min} = \sqrt{\frac{2 \cdot W}{\rho \cdot S \cdot c_{Lmax}}} = 5,01 \frac{m}{s} = 18,03 \text{ km/h} \quad (2)$$

-landing speed for $C_{Lmax}=1,77$ ($\text{AoA}=9^\circ$ and flap at 25°):

$$V_{TO} = 1,2 \cdot V_{min} = 6,01 \frac{m}{s} = 21,63 \text{ km/h} \quad (3)$$

- gliding speed for $C_L=0,55$ ($\text{AoA}=-1^\circ$):

$$V_{glide} = \sqrt{\frac{2 \cdot \cos\theta \cdot W}{\rho \cdot S \cdot c_L}} = 8,99 \frac{m}{s} = 32,36 \text{ km/h}$$

b. aerodynamic forces estimated:

-lifting for speed $8,4 \text{ m/s}$ and $C_L=0,75$ ($\text{AoA}=0^\circ$), for NACA 6409 airfoil

$$L = \frac{1}{2} \cdot \rho \cdot V^2 \cdot S \cdot c_L = 116,68\text{N} = 11,89\text{kgf} \quad (4)$$

Which confirms the initial considerations about estimating the total weight of 10 kg .

-drag estimated, $C_D=0,02$ ($\text{AoA}=0^\circ$), for NACA 6409 airfoil.

$$D = \frac{1}{2} \cdot \rho \cdot V^2 \cdot S \cdot c_D = 3,11\text{N} = 0,31\text{kgf} \quad (5)$$

-lift to drag ratio (gliding rate) estimated:

$$f = \frac{L}{D} = 37,51 \quad (6)$$

-range estimated:

$$E = \frac{R}{V} = 251\text{km} \quad (7)$$

Table 4.2. Estimated performances ATMOS-2CB

Performances	Value	Performances	Value
Cruise speed	30 km/h	Payload	2 kg
Minim speed	18 km/h	Autonomy	8h
Max weight	10 kg	Range	251 km

4.4. Mass and balancer UAV ATMOS-2CB

The mass configuration is based on the estimated values of the structure and masses of the onboard equipment, according to table 4.3. and inertia in annex 1 (mass index 2/line 3).

Table 4.3. Estimated mass ATMOS-2CB

Components	Mass	Components	Mass
Body (with payload)	5,4 kg	Fin	0,3 kg
Main wing	2,0 kg	Engine (left/right)	2 kg
Elevator	0,3 kg		

4.5. Technical aspects

The ATMOS motor glider presented in two aerodynamic configurations is built in a modular concept (9 construction elements) with elements and quick-connect for facilitate containerized transport to minimized dimensions (approximately 220 mm length), see figure 4.3. The materials used for manufacturing include composite elements but also flexible primary products EPS / XPS (extruded / expanded polystyrene), see figure 4.3.

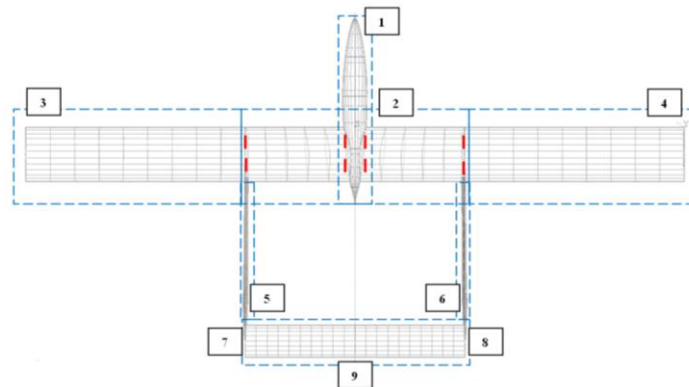


Fig. 4.3. Modular concept: (1) front fuselage; (central wing in front fuselage); (3), (4) extremal wings; (5), (6) fuselage tubes; (7), (8) vertical tails; (9) horizontal tail

5. Aerodynamic analysis

5.1. 2D aerodynamic analysis (airfoils)

5.1.1. Conditions of analysis

The aerodynamic analysis of the airfoils used on the wing (fig 4.2) has the initial conditions from table 5.1.

Table 5.1. Conditions of analysis

Condition	Value	Condition	Value
AoA range	$-5^\circ \div 15^\circ$	Nr Reynolds	100000
Air density	$1,225 \text{ kg/m}^3$	Iteration	1000

5.1.2. Results analysis

The performance of the airfoils (for wing) is highlighted with the polars C_l vs AoA and C_d vs AoA.

Gliding coefficient: NACA 6409 has $C_{l_{\max}}=1.49$ for $\text{AoA}=9^\circ$ and NACA 2409 has $C_{l_{\max}}=1.10$ for $\text{AoA}=10^\circ$, see figure 5.1 and figure 5.2. Drag coefficient: NACA 6409 has $C_{d_{\min}}=0,018$ for $\text{AoA}=2^\circ$ and NACA 2409 has $C_{d_{\min}}=0,013$ for $\text{AoA}=-2^\circ$. For the proposed airfoils, we have optimal aerodynamic performance in the range of $\text{AoA}=9 \div 10^\circ$.

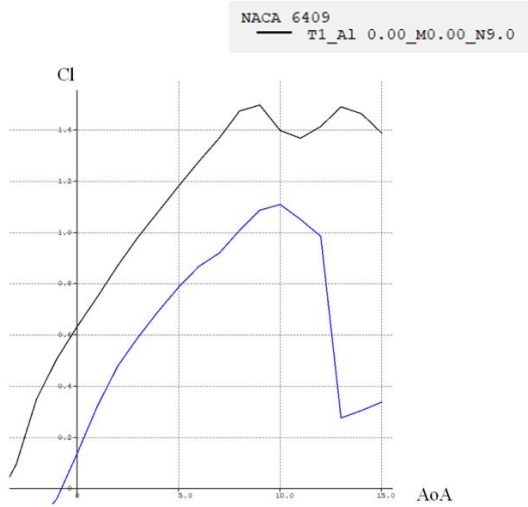


Fig. 5.1 Cl vs AoA

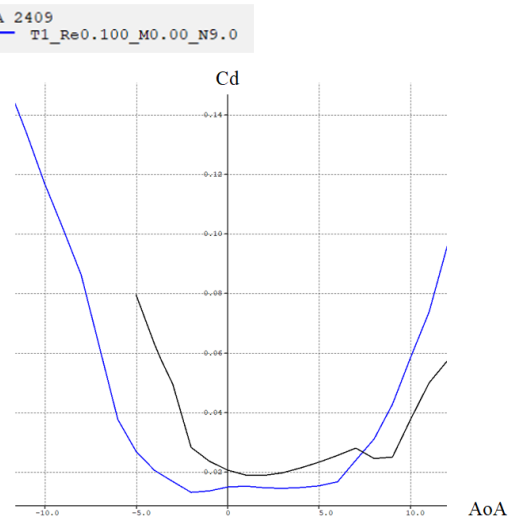


Fig. 5.2 Cd vs AoA

5.2. 3D aerodynamic analysis ATMOS-2CB

5.2.1. Conditions of analysis

To confirm the numerical results regarding flight performance, we perform an aerodynamic analysis according to the analysis conditions in table 5.1. The aerodynamic analysis was performed at the minimum gliding speed without considering the interference effects of the propellers.

Table 5.1. Conditions of analysis

Condition	Value	Condition	Value
Speed analysis	9 m/s	Nr Reynolds	300000
Air density	1,225 kg/m ³	Iteration	1000
Flight slide angle	0°	Boundary conditions	Dirichlet
AoA range	-5° ÷ 15°	Analysis method	VLM (vortex lattice method)

5.2.2. Results analysis

The minimum fuel consumption for a maximum endurance is indicated by $\sqrt{Cl^3/Cd^2}$ see figure 5.3, we have a maximum value of this parameter for $AoA=4^\circ$.

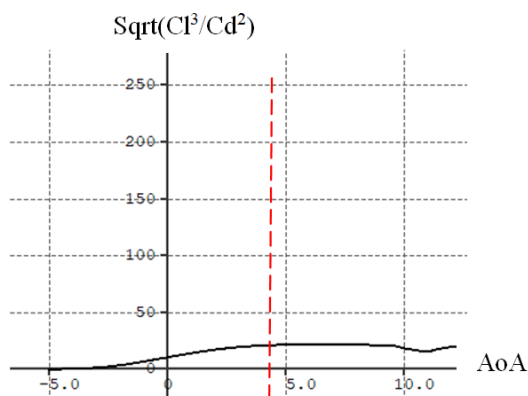


Fig. 5.3. Maximum endurance parameter

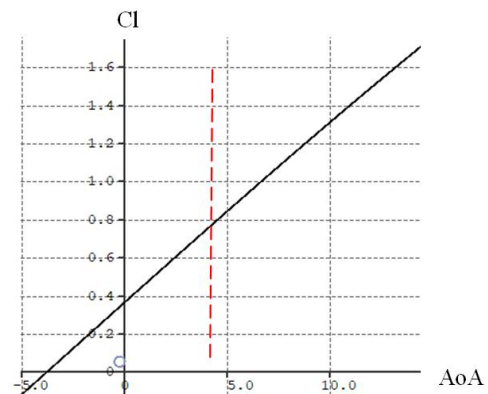


Fig. 5.4. Cl vs AoA

For maximum endurance, to understand the aerodynamic performance versus AoA we can observe the values of the lifting coefficient ($C_l=0,746$ for $AoA=4^\circ$), see figure 5.4, drag coefficient ($C_d=0,031$ for $AoA=4^\circ$) from figures 5.5, pitch coefficient ($C_m=-0,044$ for $AoA=4^\circ$) see figure 5.6 and annex 2.

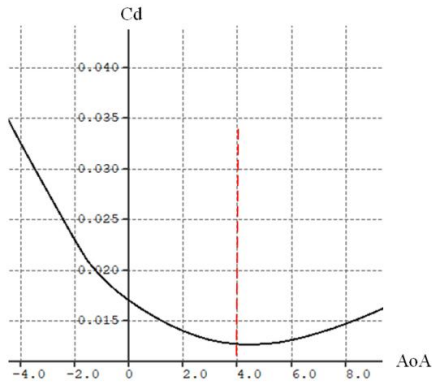


Fig. 5.5. Cd vs AoA

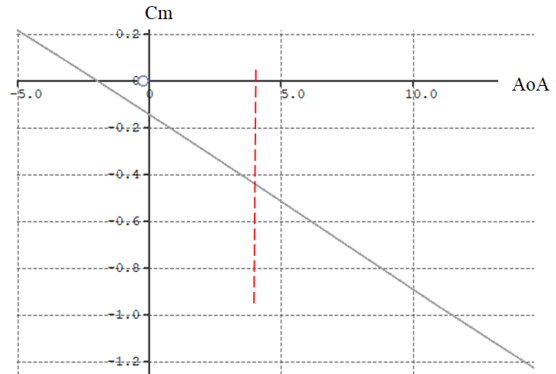


Fig. 5.6. Cm vs AoA

For horizontal flight the parameters and aerodynamic coefficients calculated with XFLR5 are highlighted in table 5.2 and annex 2.

Table 5.2. Horizontal flight aerodynamic parameters

Parameters	Value	Parameters	Value
C_l	0,362	C_l to $C_{d_{min}} (AoA=-0,5^\circ)$	0,314
C_d	0,022	$\sqrt{C_l^3/C_d^2}$	6,86
C_m	-0,143		

Conclusions

The need to use high endurance air vectors in the conditions of specific missions of acquisition of atmospheric and environmental data, leads implicitly to a careful analysis of geometric and mass characteristics with direct implications on performance and operating limits.

The paper outlined the basics of using unmanned aerial vehicles for atmospheric and environmental monitoring missions. Of course, it is necessary to estimate the performance for UAV concept with the help of software tools for an accurate prediction and for possible optimizations of the geometric characteristics and flight performances.

The limitations of aerodynamic analyzes are based on the use of VLM numerical codes, for the next stage, the use of CFD software tools is proposed.

The aerodynamic analyzes in this paper provide useful numerical benchmarks for the pre-design phase of a UAV, which can be confirmed with possible tests in wind tunnels.

The paper presented a simplified geometric configuration of a glider engine that was analyzed at the minimum flight speed to estimate the critical aerodynamic performance at the characteristic angles of attack (0° and 4°), the numerical data obtained can be used in the subsequent stages of CFD analyzes or tests experimental in the wind tunnel.

Future study directions will focus on mass and aerodynamic software optimizations to minimize total flight weight and reduce drag, both by selecting optimized aerodynamic profiles and the most efficient propulsion systems.

Acknowledgment

This article was produced with the support of the *Henri Coandă* Air Force Academy and the documentation of the international project, acronym SUSCAP-1, PN-III-COFUND-SUSCROP-SUSCAP-1, contract 106/2019 financed by UEFISCDI.

References

[1]	Novak, D.R., Operational Meteorology, <i>Encyclopedia of Atmospheric Sciences (Second Edition) - WEATHER FORECASTING / Operational Meteorology</i> , 293-302, 2015
[2]	Varentsov M.I., Artamonov A.Y., Pashkin A.D., Repina A.I., <i>Experience in the quadcopter-based meteorological observations in the atmospheric boundary layer</i> , IOP Conference Series: Earth and Environmental Science, Volume 231, 231 012053, 2019
[3]	Flagg D.D., Doyle J.D., Holt T.R., Tyndall, D.P, Amerault C.M., <i>On the impact of unmanned aerial system observations on numerical weather prediction in the coastal zone</i> . Monthly Weather Review, volume 146, 599-622, 2018
[4]	Sun Q., Vihma T, Jonassen M.O., Zhang Z., <i>Impact of Assimilation of Radiosonde and UAV Observations from the Southern Ocean in the Polar WRF Model</i> , Advances In Atmospheric Sciences, Volume 37, 441-454, 2020.
[5]	Manfreda S., McCabe M.F., Miller P. E., et al, <i>On the use of unmanned aerial systems for environmental monitoring</i> , Remote sensing, Volume 10, 641, 2018
[6]	Cook D.E., Strong P.A., Garret S.A., Marshall R.E., <i>A small unmanned aerial system (UAS) for coastal atmospheric research: preliminary results from NewZealand</i> , Journal of the Royal Society of New Zealand, Volume 43, 108-115, 2013
[7]	Rohi G., Ejofodomi O., Ofualagba G., <i>Autonomous monitoring, analysis, and countering of air pollution using environmental drones</i> , Heliyon, Volume 6, e03252, 2020
[8]	Gu Q., Michanowicz D.R., Jia C., <i>Developing a modular unmanned aerial vehicle(UAV) platform for air pollution profiling</i> , Sensors, Volume 18, 4363, 1–14, 2018
[9]	Ruiz-Jimenez J., Zanca N., Lan H., Jussila M., Hartonen K., <i>Aerial drone as a carrier for miniaturized air sampling systems</i> , J. Chromatogr. A, 1597, 202–208, 2019
[10]	Prisacariu V., Cheval S., <i>Using UAV-LTA for environmental monitoring</i> , Air and Water – Components of the Environment” Conference Proceedings 2019, 22-24 martie 2019, Editura Universitatea Babeş-Bolyai Cluj-Napoca, ISSN 2067-743X, p.39-52, doi 10.24193/AWC2019_05
[11]	Prisacariu V., Cioacă C. Boşcoianu M. <i>Analysis performances of UAV airships</i> , Scientific Bulletin of Naval Academy, ISSN : 2392-8956 ; ISSN-L : 1454-864X, vol 21. 1/2018, p.180-189, doi 10.21279/1454-864X-18-I1-030, MBNA Publishing House Constanta 2018, presented at SEACONF 2018 Constanța
[12]	Nelson Javier Pedraza Betancourth, Julio Enoc Parra Villamarin, John Jairo Vaca Rios, Pedro David Bravo-Mosquera, Hernán Darío Cerón-Muñoz, <i>Design and manufacture of a solar-powered unmanned aerial vehicle for civilian surveillance missions</i> , Journal of Aerospace Technology and Management, vol. 8 (4), Oct-Dec 2016, https://doi.org/10.5028/jatm.v8i4.678
[13]	<i>Meteomatics multicopter</i> , https://www.meteomatics.com/en/meteodrones-technology , accessed at 20.03.2022
[14]	Ventura D., Bonifazi A., Gravina M. F., and Ardizzone G., <i>"Unmanned Aerial Systems (UASs) for Environmental Monitoring: A Review with Applications in Coastal Habitats"</i> , in Aerial Robots - Aerodynamics, Control and Applications. London, United Kingdom: IntechOpen, 2017 [Online]. https://www.intechopen.com/chapters/55936 doi: 10.5772/intechopen.69598
[15]	Anderson K., Gaston K.J. <i>Lightweight unmanned aerial vehicles will revolutionize spatial ecology</i> . Frontiers in Ecology and the Environment. 2013;11(3):138-146. DOI: 10.1890/120150
[16]	Marcaccio J.V., Markle C.E., Chow-Fraser P., <i>Use of fixed-wing and multi-rotor unmanned aerial vehicles to map dynamic changes in a freshwater marsh</i> . Journal of Unmanned Vehicle Systems. 2016;4(3):193-202. DOI: 10.1139/juvs-2015-0016
[17]	Chabot D., Bird D. M., <i>Small unmanned aircraft: precise and convenient new tools for surveying wetlands</i> , 2013, Journal of Unmanned Vehicle Systems, p. 15-24, Vol.1, 01, doi: 10.1139/juvs-2013-0014, https://cdnsiencepub.com/doi/abs/10.1139/juvs-2013-0014

[18]	Hodgson A, Kelly N, Peel D., <i>Unmanned aerial vehicles (UAVs) for surveying marine fauna: A dugong case study</i> . PloS One. 2013;8(11):e79556. DOI: 10.1371/journal.pone.0079556
[19]	Watts A.C., Ambrosia V.C., and Hinkley E.A., 2012. <i>Unmanned aircraft systems in remote sensing and scientific research: classification and considerations of use</i> . Remote Sens 4: 1671–92.
[20]	<i>XFLR5 Analysis of foils and wings operating at low Reynolds numbers</i> , 58p, 2009, disponible at https://engineering.purdue.edu/~aerodyn/AAE333/FALL10/HOMEWORKS/HW13/XFLR5_v6.01_Beta_Win32%282%29/Release/Guidelines.pdf , accesat la data de 12.03.2022
[21]	https://www.rc-zeppelin.com/outdoor-rc-blimps-5m.html , accessed at 18.03.2022
[22]	Pieri, David & Diaz, Jorge & Bland, Geoff & Fladeland, Matthew & Madrigal, Yetty & Corrales, Ernesto & Alegria, Oscar & Alan, Alfredo & Realmuto, Vincent & Miles, Ted & Abtahi, Ali. (2013). <i>In situ observations and sampling of volcanic emissions with NASA and UCR unmanned aircraft, including a case study at Turrialba Volcano, Costa Rica</i> . Geological Society of London Special Publications. 380. 321-352. 10.1144/SP380.13.
[23]	https://sinovoltaics.com/technology/top8-leading-companies-developing-solar-powered-drone-uav-technology/ , accessed at 20.03.2022
[24]	Ball M., <i>Silent Falcon Selected by DARPA for Laser-Powered UAS Project</i> , 2018, disponibil la https://www.unmannedsystemstechnology.com/2018/08/silent-falcon-selected-by-darpa-for-laser-powered-uas-project/ , accessed at 19.03.2022
[25]	<i>URAD monitor datasheet - Environmental Monitoring</i> , product manual – Advanced air quality monitoring station, 11p., available at https://www.uradmonitor.com/wordpress/wp-content/uploads/2017/02/datasheet_a3.pdf , accessed at 19.03.2022
[26]	https://www.uradmonitor.com/ , accessed at 19.03.2022
[27]	<u>Keskin, G., Durmus, S., Karakaya, M. and Kushan, M.C. (2021), "Designing and producing a bird-inspired unmanned sailplane", <i>Aircraft Engineering and Aerospace Technology</i>, Vol. 93 No. 6, pp. 1052-1059. https://doi.org/10.1108/AEAT-02-2021-0054</u>
[28]	Sniffer 4D – specification, 2020, http://sniffer4d.eu/wp-content/uploads/2020/01/Public_Sniffer4D_Specifications.pdf , accessed at 21.03.2022
[29]	Karthik Reddy Buchireddy Sri, Poondla Aneesh, Kiran Bhanu, M. Natarajan, <i>Design analysis of solar-powered unmanned aerial vehicle</i> , Journal of Aerospace. Technology and Management, vol. 8 (4), Oct-Dec 2016, https://doi.org/10.5028/jatm.v8i4.666

Annex 1. Mass and inertia

mass	x	y	z	Ixx	Iyy	Izz	Ixy	Ixz	Iyz	
2	211	1.43e-13	33	5.99e+06	2.92e+04	6.02e+06	0	129	0	! ATMOS-2CB Combustie bimotor_wing
0.3	1.93e+03	5.08e-14	410	1e+05	1.49e+03	1.01e+05	0	-2.14e-23	0	! ATMOS-2CB Combustie bimotor_wing2
2	81.4	2.69e-13	0	2e+06	1.61e+04	2.02e+06	0	0	0	! ATMOS-2CB Combustie bimotor_engine
0.3	1.7e+03	-3.48e-14	166	3.04e+05	1.4e+04	3.1e+05	0	-3.21e+03	0	! ATMOS-2CB Combustie bimotor_Fin
5.4	-412	0	-5.61	1.11e+03	8.16e+05	8.15e+05	0	-2.53e+04	0	! Body's inertia

Annex 2. Aerodynamic parameters

Plane name : ATMOS-2CB Mk2 Combustie bimotor												
Polar name : T1-9.0 m/s-VLM2												
Freestream speed : 9.000 m/s												
-1.000	0.000	0.265868	0.003284	0.019284	0.022568	0.000000	0.000000	-0.070422	-0.000000	-0.000000	9.0000	0.1339
-0.500	0.000	0.314237	0.004207	0.018009	0.022216	0.000000	0.000000	-0.106992	-0.000000	-0.000000	9.0000	0.1714
0.000	0.000	0.362569	0.005284	0.016961	0.022245	0.000000	0.000000	-0.143694	-0.000000	-0.000000	9.0000	0.1990
0.500	0.000	0.410857	0.006515	0.016060	0.022575	0.000000	0.000000	-0.180519	-0.000000	-0.000000	9.0000	0.2200
1.000	0.000	0.459093	0.007898	0.015262	0.023160	0.000000	0.000000	-0.217461	-0.000000	-0.000000	9.0000	0.2367
1.500	0.000	0.507269	0.009434	0.014532	0.023966	0.000000	0.000000	-0.254507	-0.000000	-0.000000	9.0000	0.2502
2.000	0.000	0.555377	0.011121	0.013936	0.025057	0.000000	0.000000	-0.291652	-0.000000	-0.000000	9.0000	0.2613
2.500	0.000	0.603411	0.012958	0.013426	0.026384	0.000000	0.000000	-0.328882	-0.000000	-0.000000	9.0000	0.2708
3.000	0.000	0.651362	0.014944	0.013029	0.027973	0.000000	0.000000	-0.366190	-0.000000	-0.000000	9.0000	0.2788
3.500	0.000	0.699222	0.017079	0.012774	0.029853	0.000000	0.000000	-0.403564	-0.000000	-0.000000	9.0000	0.2857
4.000	0.000	0.746985	0.019360	0.012628	0.031988	0.000000	0.000000	-0.440993	-0.000000	-0.000000	9.0000	0.2918